

Supporting Information

Photovoltaic Modulation of Ferromagnetism within FM Metal/P-N Junction Si Heterostructure

Yifan Zhao^{#,1}, Shishun Zhao^{#,1}, Lei Wang^{#,3}, Shiping Wang⁴, Yujing Du¹, Yanan Zhao¹, Shengye Jin⁴, Tai Min³, Bian Tian,² Zhuangde Jiang,² Ziyao Zhou¹, Ming Liu^{,1}*

1. Electronic Materials Research Laboratory, Key Laboratory of the Ministry of Education & International Center for Dielectric Research, School of Electronic and Information Engineering, and State Key Laboratory for Mechanical Behavior of Materials, the International Joint Laboratory for Micro/Nano Manufacturing and Measurement Technology, Xi'an Jiaotong University, Xi'an 710049, China

2. State Key Laboratory for Manufacturing Systems Engineering, Collaborative Innovation Center of High-End Manufacturing Equipment, the International Joint Laboratory for Micro/Nano Manufacturing and Measurement Technology, Xi'an Jiaotong University, Xi'an 710049, China

3. Center for Spintronics and Quantum System, State Key Laboratory for Mechanical Behavior of Materials, School of Materials Science and Engineering, Xi'an Jiaotong University, Xi'an, Shaanxi, 710049, China

4. State Key Laboratory of Molecular Reaction Dynamics and Collaborative Innovation Center of Chemistry for Energy Materials (iChEM), Dalian Institute of Chemical Physics, Chinese Academy of Sciences, 457 Zhongshan Rd., Dalian, 116023, China.

These authors contributed equally to this work.

*E-mail: mingliu@xjtu.edu.cn

Supplementary Experiment

1. Pristine Si wafer with p - n junction in situ ESR measurement.

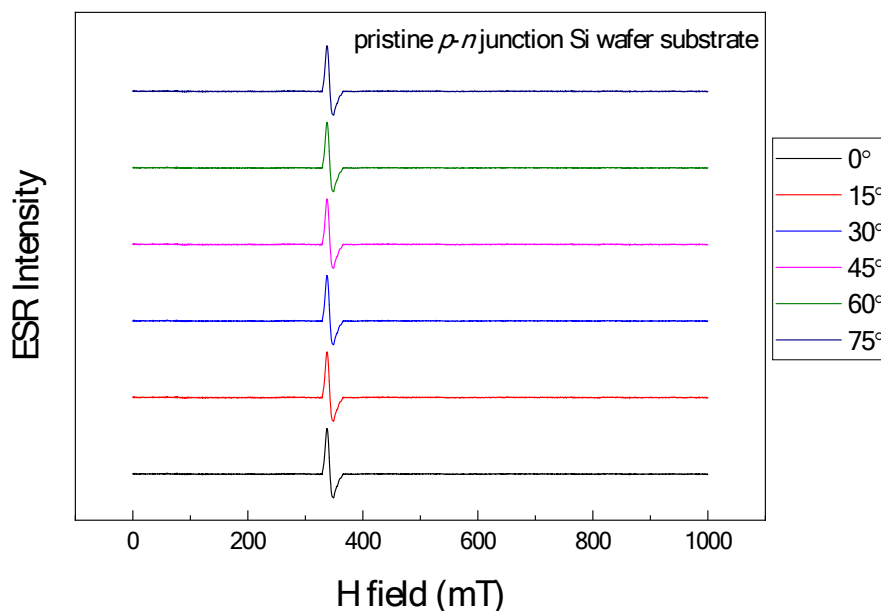


Figure S1. The pristine Si wafer with p - n junction in ESR measurement at different degrees.

2. ESR test and spectrums of Magnetic Anisotropy Change of Co under Temperature Effect

To quantitatively determine the temperature effect, a thermocouple was supposed to get contacted with the sample in the ESR cavity during the measurement. However, loading a thermocouple into the cavity enables a huge microwave loss so that the magnetic signal is too weak to be detected. Therefore, we carried out a control experiment to evaluate the temperature effect. In the beginning, a thermometer was used to precisely determine the maximum temperature change under a certain illumination intensity. The bulb of the thermometer was blackened before the test.

During the evaluation, the irradiation time was long enough to ensure the temperature was stable. Finally, we found the temperature was changed from room temperature to 39.6 °C with the illumination of 140 mW cm⁻². We assumed that the sample also underwent such thermal influence with sunlight illumination.

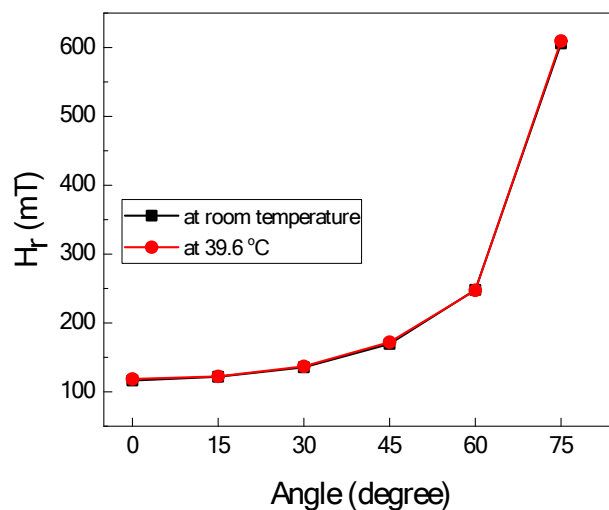


Figure S2. Angular dependence of the photovoltaic induced ferromagnetic resonance field shift with 3 nm Co layer on Si wafer with a *p-n* junction at room temperature and 39.6 °C, respectively.

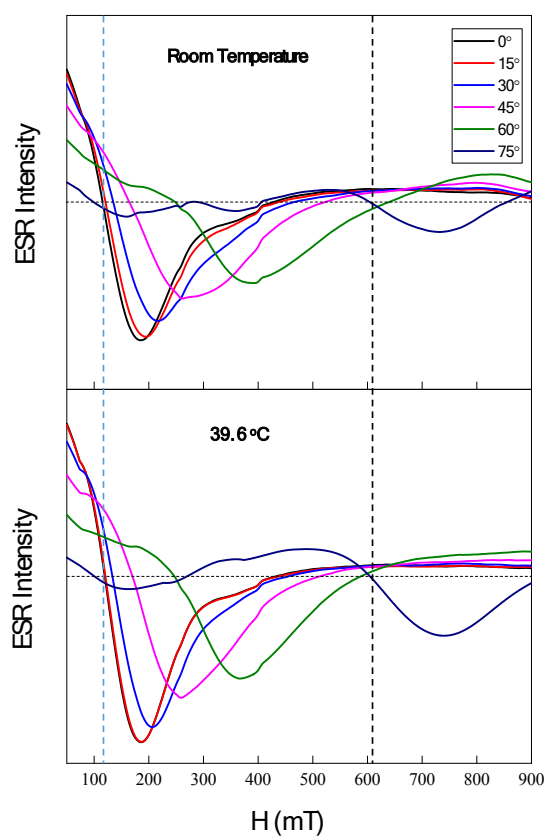


Figure S3. ESR spectrums of 3 nm Co on Si wafer with a *p-n* junction at room temperature and 39.6 °C without light illumination, respectively.

3. Comparison of the Magnetic Anisotropy Change of different thickness of Co films without light illumination.

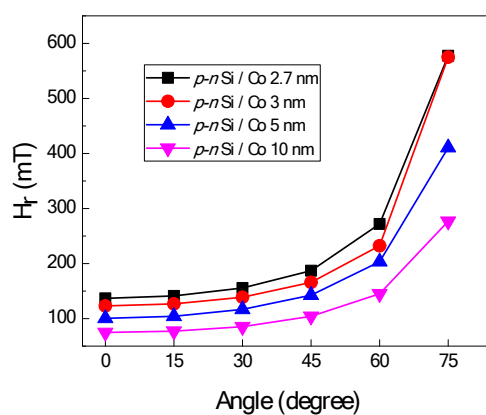


Figure S4. Angular dependence of the photovoltaic induced ferromagnetic resonance field shift with 2.7, 3, 5, and 10 nm Co layer without light illumination, respectively.

4. Variation of ΔH_r under 0.6 sun Intensity of Illumination with 2.7, 3, 5, 10 nm Co layer

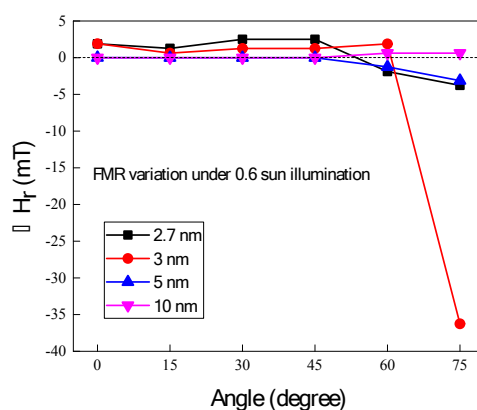


Figure S5. The angular dependence of the FMR field under 0.6 sun intensity of light illumination for the 2.7 nm, 3 nm, 5 nm, and 10 nm Co samples, respectively.

5. Variation of H_r under Different Intensities of Illumination with 3, 5, 10 nm Co layer, respectively.

The devices with different thicknesses of the Co layer were also fabricated on the Si wafer with *p-n* junction and tested. The results of the angular dependence of the photovoltaic induced FMR field shifts are shown in Figure S6 ~ S8, respectively. From Figure S6, there are distinct variations of the FMR field under the different illumination of visible light. However, the FMR field shift is hardly observed, with the thickness of

Co increasing. As shown in Figure S7 and S8, the field shift of FMR cannot be obtained with 5 nm and 10 nm Co layer.

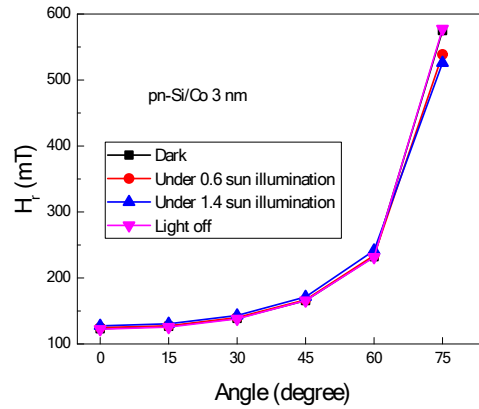


Figure S6. Angular dependence of the photovoltaic induced ferromagnetic resonance field shift with 3 nm Co layer.

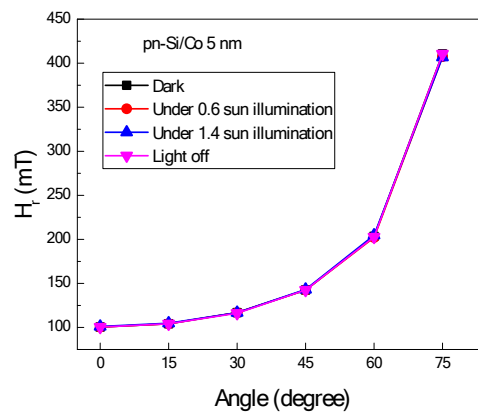


Figure S7. Angular dependence of the photovoltaic induced ferromagnetic resonance field shift with 5 nm Co layer.

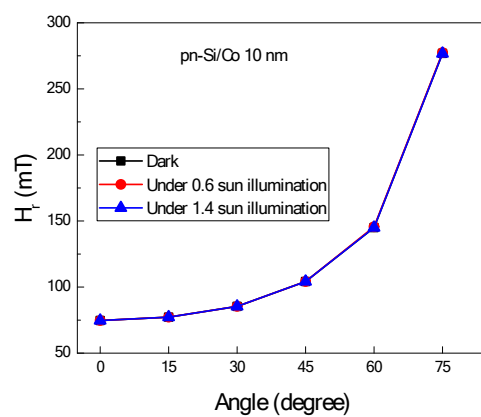


Figure S8. Angular dependence of the photovoltaic induced ferromagnetic resonance field shift with 10 nm Co layer.

6. ESR test of Magnetic Anisotropy Change under Different Intensities of Illumination with 2.7, 3, 5, 10 nm of Co Layer.

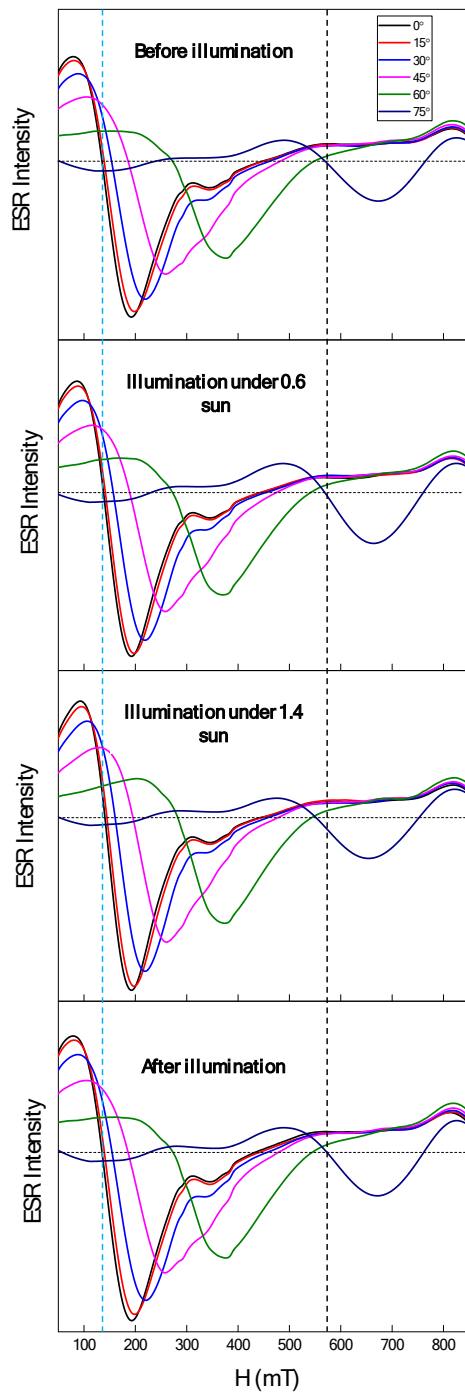


Figure S9. ESR spectrums of in situ photovoltaic gatings with 2.7 nm Co on Si wafer with *p-n* junction before and after light illumination

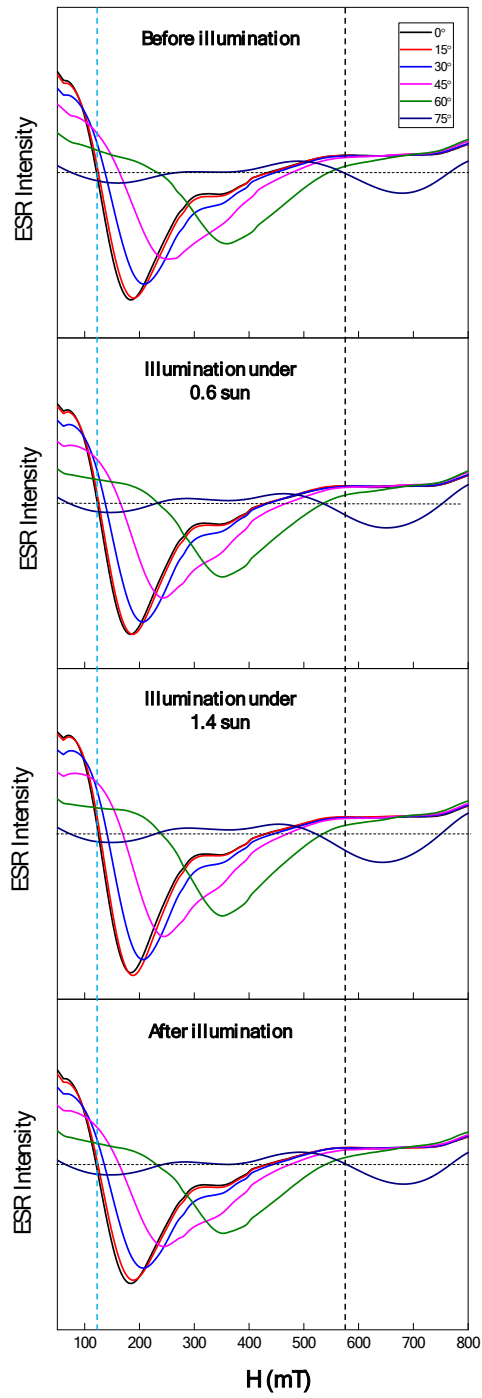


Figure S10. ESR spectrums of in situ photovoltaic gatings with 3 nm Co on Si wafer with p - n junction before and after light illumination

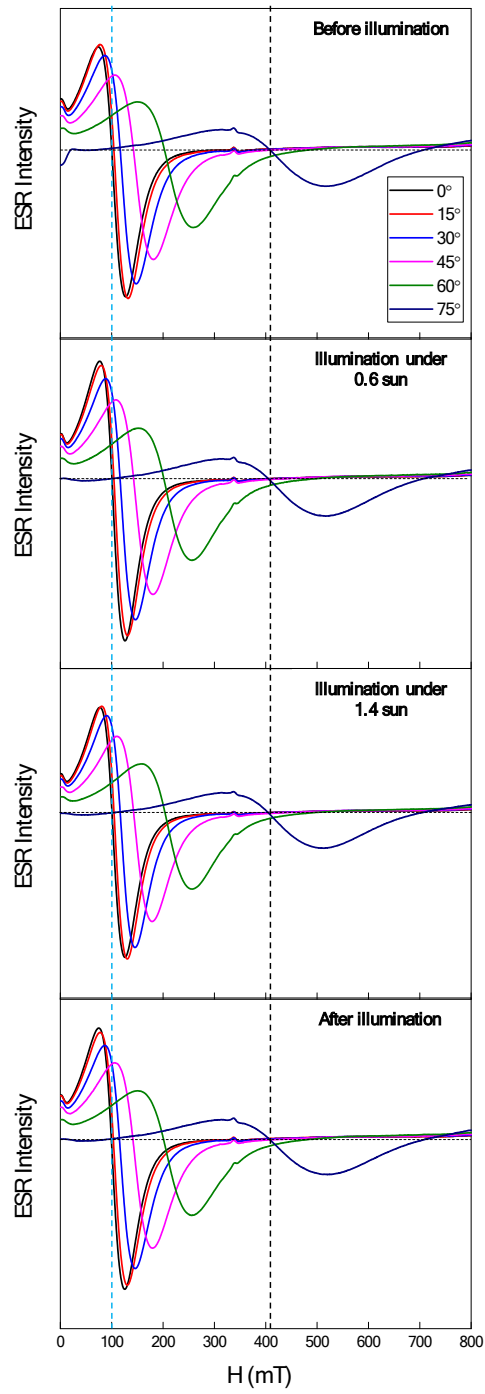


Figure S11. ESR spectrums of in situ photovoltaic gatings with 5 nm Co on Si wafer with p - n junction before and after light illumination

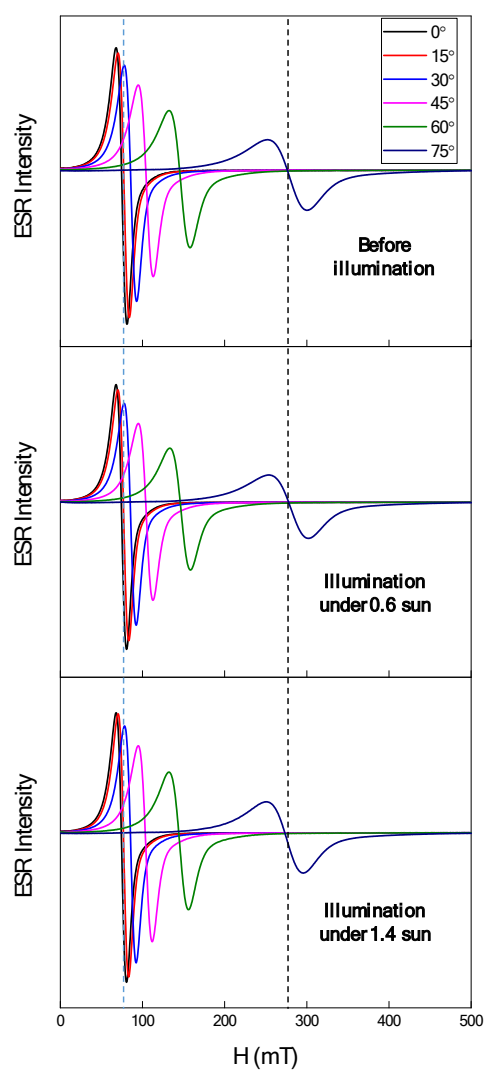


Figure S12. ESR spectrums of in situ photovoltaic gatings with 10 nm Co on Si wafer with p - n junction before and after light illumination

7. ESR test and spectrums of Magnetic Anisotropy Change of CoFeB under Temperature Effect

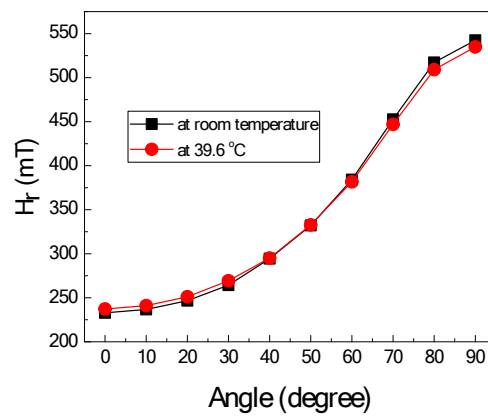


Figure S13. Angular dependence of the photovoltaic induced ferromagnetic resonance field shift with 1.5 nm CoFeB layer on Si wafer with a *p-n* junction at room temperature and 39.6 °C, respectively.

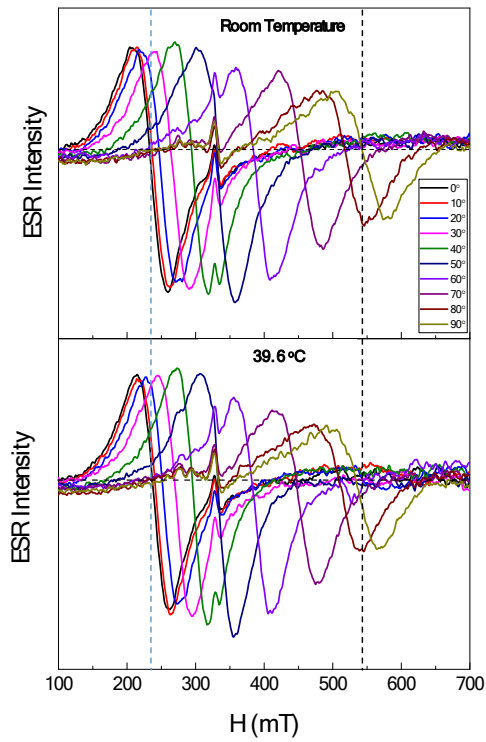


Figure S14. ESR spectrums of 1.5 nm CoFeB on Si wafer with a *p-n* junction at room temperature and 39.6 °C without light illumination, respectively.

8. Comparison of the Magnetic Anisotropy Change of different thickness of CoFeB films without light illumination.

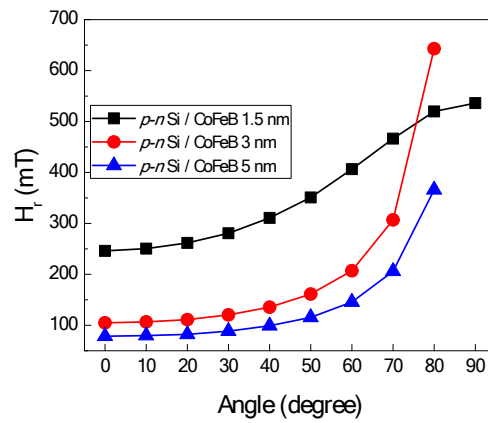


Figure S15. Angular dependence of the photovoltaic induced ferromagnetic resonance field shift with 1.5, 3, and 5 nm CoFeB layer without light illumination, respectively.

9. Variation of ΔH_r under 0.6 sun Intensity of Illumination with 1.5, 3 and 5 nm CoFeB layer

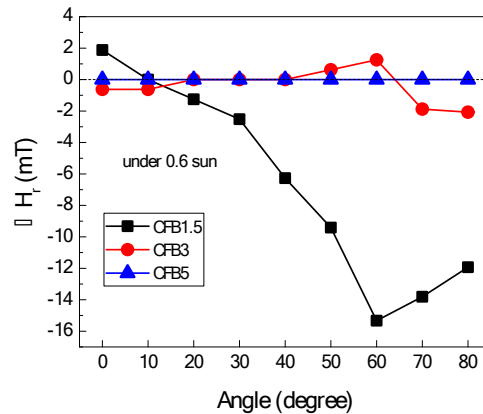


Figure S16. The angular dependence of the FMR field under 0.6 sun intensity of light illumination for the 1.5 nm, 3 nm, and 5 nm CoFeB samples, respectively.

10. Variation of H_r under Different Intensities of Illumination with 1.5, 3, 5 nm CoFeB layer, respectively.

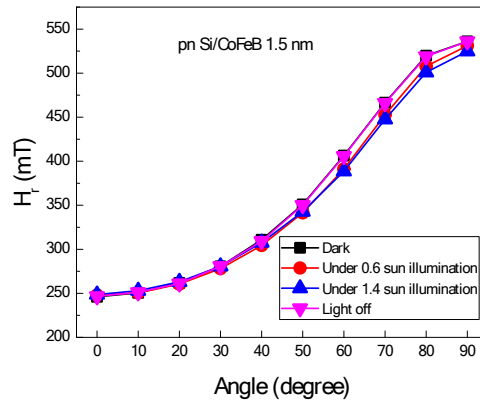


Figure S17. Angular dependence of the photovoltaic induced ferromagnetic resonance field shift with 1.5 nm CoFeB layer.

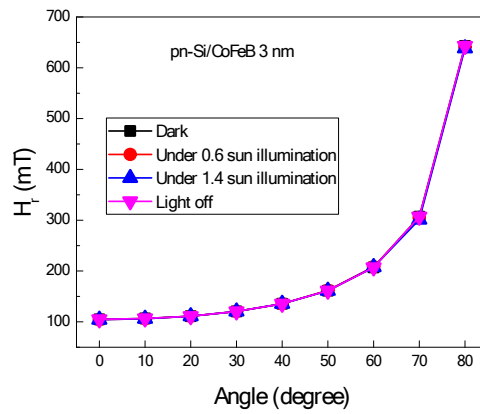


Figure S18. Angular dependence of the photovoltaic induced ferromagnetic resonance field shift with 3 nm CoFeB layer.

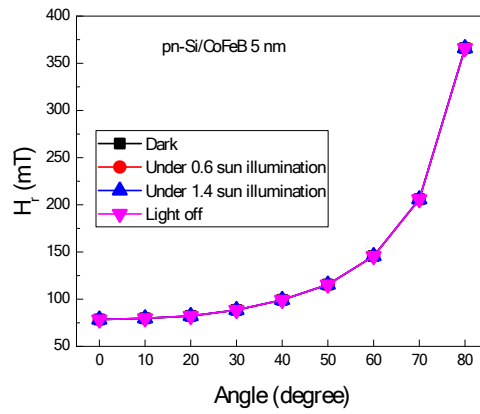


Figure S19. Angular dependence of the photovoltaic induced ferromagnetic resonance field shift with 5 nm CoFeB layer.

11. ESR test of Magnetic Anisotropy Change under Different Intensities of Illumination with 1.5, 3, 5 nm CoFeB layer.

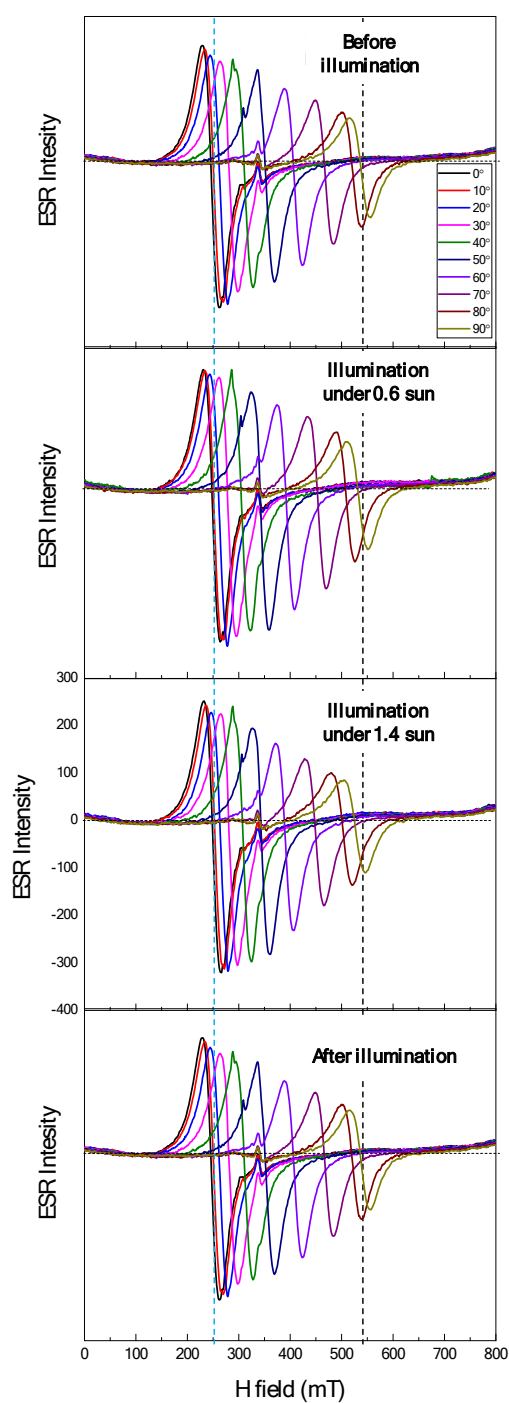


Figure S20. ESR spectrums of in situ photovoltaic gatings with 1.5 nm CoFeB on Si wafer with p - n junction before and after light illumination.

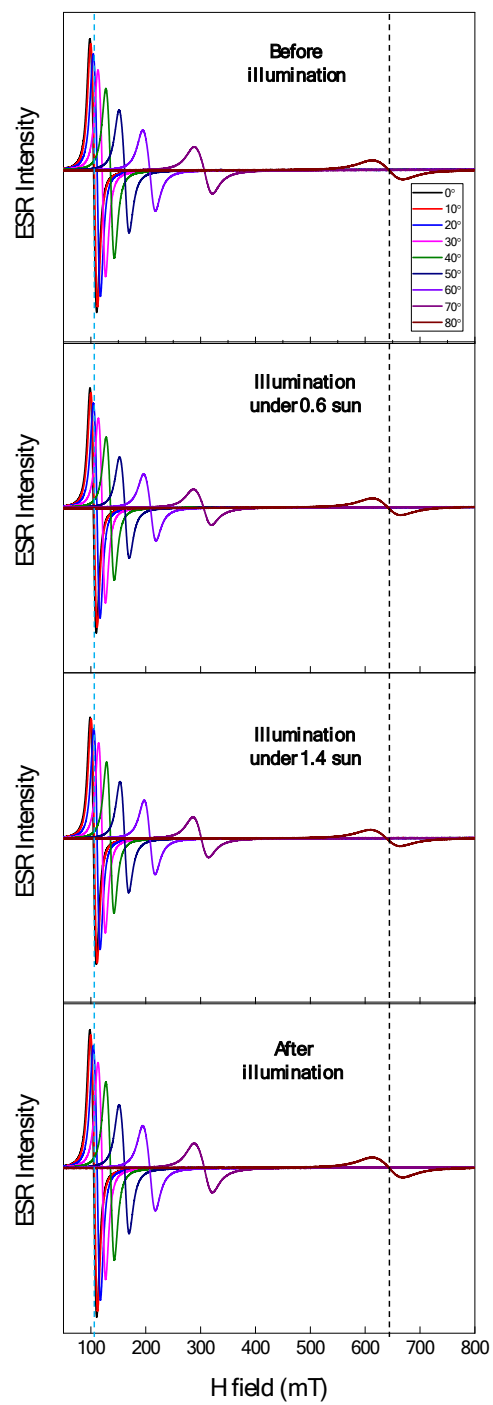


Figure S21. ESR spectrums of in situ photovoltaic gatings with 3 nm CoFeB on Si wafer with *p-n* junction before and after light illumination.

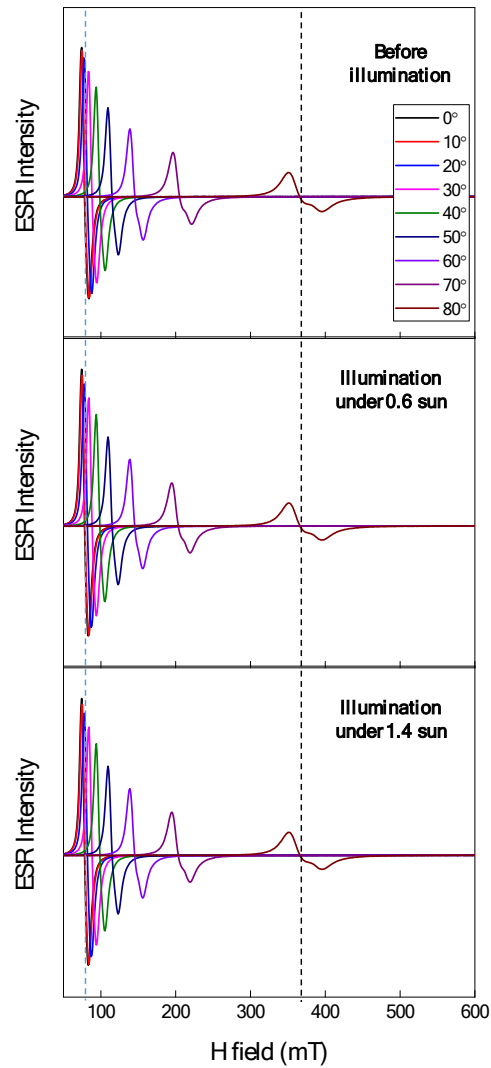


Figure S22. ESR spectrums of in situ photovoltaic gatings with 5 nm CoFeB on Si wafer with *p-n* junction before and after light illumination.

12. FMR field shift of photovoltaic gating with 3 nm Co on Si wafer without *p-n* junction in situ ESR measurement

A very little signal difference in Co on Si wafer without *p-n* junction was caused by the temperature effect under visible light illumination. During the visible light illumination with the illumination of 140 mW cm^{-2} , the temperature was changed from room temperature to $39.6 \text{ }^\circ\text{C}$. We found that there were very little difference in location

of FMR field induced by temperature effect on Si wafer without p-n junction (shown in Figure S23) compared with the results by the photo-induced electrons doping on p-n Si wafer (shown in Figure S10). It is consistent with our results shown in Figure 2d. Therefore, this subtle change on the FMR field location on Si wafer without p-n junction is caused by the temperature effect under the visible light illumination.

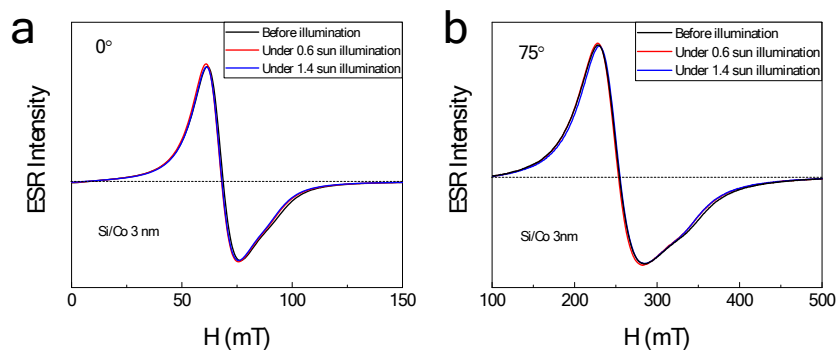


Figure S23. Photovoltaic gating of 3 nm Co on Si wafer without *p-n* junction in situ ESR measurement under the different intensity of light illumination: a) at 0 degree and b) at 75 degrees.

13. Transient Reflection Spectrums Test

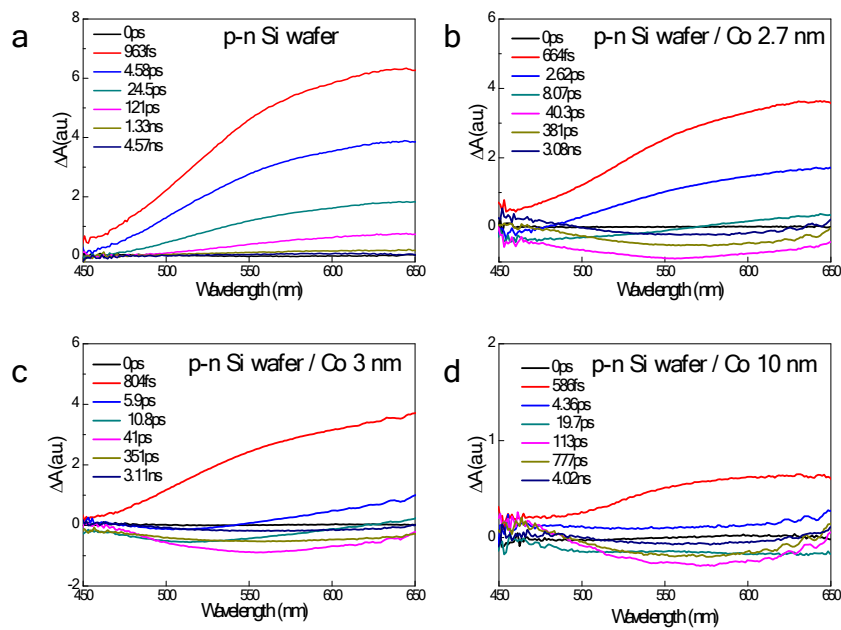


Figure S24. Transient reflection (TR) spectra of *p-n* Si wafer with different thickness of Co film. a) pristine Si wafer with a *p-n* junction. b) Si wafer with a *p-n* junction with 2.7 nm Co film. c) Si wafer with a *p-n* junction with 3 nm Co film. d) Si wafer with a *p-n* junction with 10 nm Co film. The excitation wavelength is 600 nm, with a power of $7 \mu\text{J}/\text{cm}^2/\text{pulse}$.

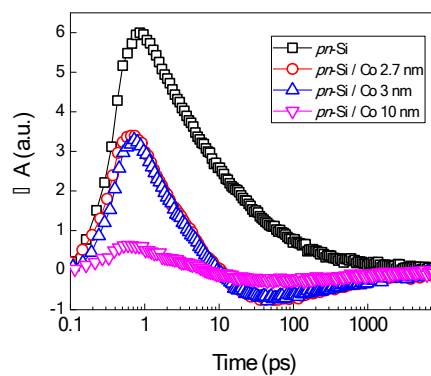
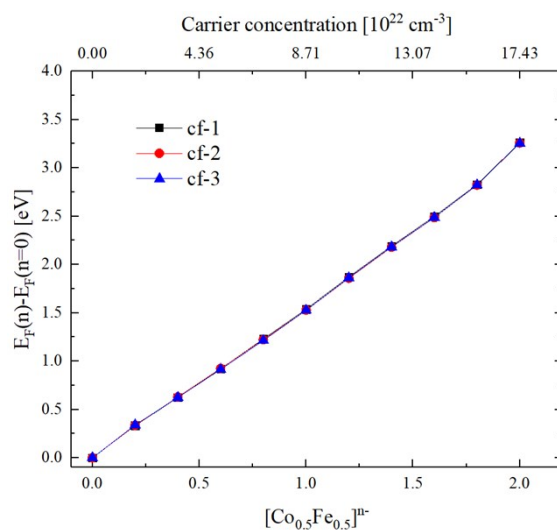


Figure S25. The comparison of TR Kinetics probed at 650 nm.

14. Fermi energy shift and the carrier concentration

As the Fermi level shift and the carrier concentration were also important for clear view of the carrier doping effect, we plotted the corresponding data in Figure S26, where we only showed the changing of the Fermi energy referring to the CoFe without



any carrier ($E_F(n) - E_F(n=0)$).

Figure S26. The Fermi level shift induced by carrier doping and the corresponding carrier concentration.